DIC method applied in the calibration of FEA model of rock-mortar cohesive interface detachment

Edivaldo J. S. Junior[1], Aref K. L. Kzam[2], Julio F. Lopez[3]

[1]*Dept. of Dam Structures, Itaipu Tecnological Park*
Tancredo Neves street, No.6731, Foz do Iguaçu, 85.867-970, Paraná – Brasil
edivaldo.junior@pti.org.br
[2]*ILATIT, Federal University of Latin American Integration*
Tancredo Neves street, No.6731, Foz do Iguaçu, 85.867-970, Paraná – Brasil
aref.kzam@unila.edu.br
[3]*School of Civil Engineering, Chongqing University*
Shapingba Main Street. No. 174, Shapingba District, 400044, Chongqing, China
j.florezlopez@gmail.com

Abstract. In civil engineering, the stability of many structures depends on the physical properties of the contact between the concrete seated on the rocky foundation surface. Usually, they are critical structures of great importance to society, such as: bridges, tunnels and dams. Thus, the shear behavior of rock-concrete joints is a key factor of the structural stability. The method of cohesive zones (CZM) allows to simulate the beginning of the formation of a crack and its propagation, without knowing the crack location or when it will start. Thus, in this work, a numerical model was developed capable of simulating the failure due to interfacial delamination of the contact between a structure formed by mortar seated on a rocky granite leaning surface. The calibration of the numerical model was performed using the results of an experimental test of simple compression on a block of rock in contact with the mortar by an inclined interface. The test was monitored using a high resolution digital camera. The data were processed using the digital image correlation method (DIC) to obtain displacement and deformation data. The DIC results were used to calibrate the nonlinear numerical model of the test using the bilinear method of cohesive zone in the rock-mortar interfacial contact elements. By a parametric analysis, the parameters of the bilinear law were determined (Maximum tensile stress and critical displacement and damage rate). Indirectly, the rate of release of energy of critical deformation from the rupture of the contact was also estimated.

Keywords: Interfacial Crack, DIC, FEA, Cohesive Zone, Bilinear law, Delamination.

1 Introduction

In civil engineering, the stability of many structures depends on the physical properties of the concrete-rock contact. Usually, they are critical structures such bridges, tunnels and dams. Thus, the shear behavior of joints formed by the settlement of concrete in a rocky interface is a structural stability key factor.

Structural numerical simulation allows evaluating the linear and non-linear behavior of structures such as rock foundations at full scale due to technological advances in computation.

However, the results obtained from numerical models can be incompatible with the behavior of the real structure or experimental tests. Thus, the Digital Image Correlation method (DIC) is presented as an alternative to establish a connection the experimental tests results and numerical simulations, allowing calibration and validation of these models

The DIC method allows obtaining physical quantities through digital images, without contact the tested material.

This method allows the determination of displacements and deformations of the investigated objects, in two-dimensional (2D) and three-dimensional (3D) spaces, from high-resolution images that are recorded during a test by image pixel variation [1].

In the case of joints formed by laying concrete on rock, the adhesion occurs during the curing and hardening of the concrete creating a cohesive resistance in contact, preventing displacements.

The cohesive zone method (MZC) allows to model crack propagation and joint detachment without the need for a pre-existing crack. Cohesive zone analyzes can predict the locations and directions of early cracks or simulate complex geometries with more than one type of interface. In a ZC model, elements are placed along the materials interface. The deformation and separation of these elements under mixed-mode loading conditions are guided by tensile separation laws [2].

2 DIC –Digital Image Correlation

The DIC method is based on the analysis of successive images, which are obtained before and after the deformation of an object submitted to a load. These images are analyzed by a correlation algorithm that initially divides the reference image (without deformations) into several sections (blocks). These sections are mapped and searched by the algorithm in the following image, after deformation. Each block is formed by a unique set of pixels and the objective of the algorithm is to determine its new position after loading. For each section to be unique, the surface of the object must have a high contrast random texture across the interest area. This texture can be natural or artificial, created through random painting using different shapes and gray scales [3]. The DIC methodology has two sources of parameters that must be adjusted and calibrated, distributed in three stages of execution, as shown in Figure 1 [4].

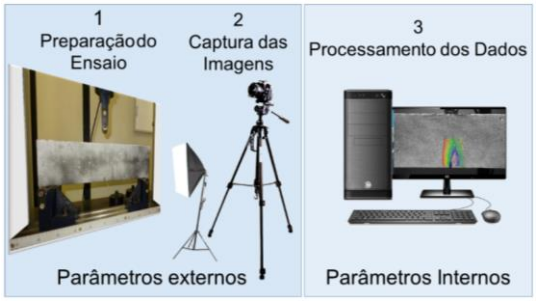

Figure 1 – Illustration of DIC steps

Basically, the analyzed interest surface of the object must present a texture allows the visualization of the material's deformation using DIC algorithms. This surface must have a random distribution of grains, high contrast and cover all gray's tone, from level 0 (black) to level 255 (white).

It is recommended to use artificial lighting to ensure the same light intensity during all test period. Because the test data is obtained through image capture, DIC processing is extremely sensitive to ambient light variation. In addition, artificial lighting helps to contract the texture, improving the accuracy of the results [5].

1.1. Images capture

The test image is captured using a high resolution digital camera. In the 2D-DIC case, a single Camera is positioned normal to the interest plane [3]. The image acquisition frequency is directly associated with the loading application time and the deformations presented by the object under analysis. The frequency of image capture must be sufficient to map the physical behavior, however, it is not desirable to have an excessive amount of images because will only increase the processing time [6]

1.2. Data Processing

From a computational point, monochromatic images have advantages in processing when compared to color images. This is because the intensity of each pixel is defined based using just one scale. In a monochrome image the gray scale ranges from level 0 (black) to 255 (white). In this way, a single matrix is capable storing this information. However, using a color image in RGB (Red-Green-Blue) format, for example, three matrices are needed to define the intensity of each pixel (red, green and blue). For this reason, many programs use only monochromatic images [6]. In Figure 2 an illustration of a grayscale image and the respective pixel matrix is presented.

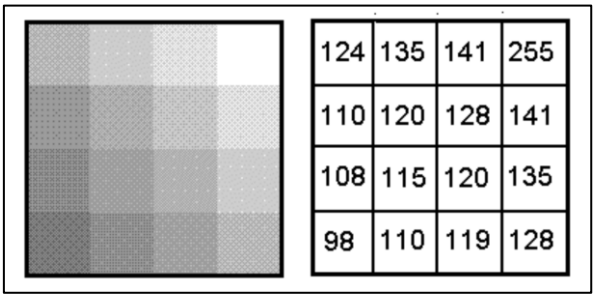

Figure 2 - Illustration of a digital image and its respective pixel matrix

After to restrict the interesting area in the reference image and realize a texture validation, it is possible to understand how the DIC algorithms perform the correlation between images through the correspondence of pixel sets, called blocks [6].

Initially, the interesting image area is divided into several small parts with an amount of pixels. Each part is called a block. Due to the randomness of the texture, each block have a unique pixel intensity matrix. Then, for each block in reference image, the algorithm look the blocks in the next image until finds the respective matrix by means of a minimization function. If the texture does not present an adequate stochastic pattern, more than one block can present the same tone intensity matrix, causing an incorrect correspondence or even a non-correlation between the images [6].

3 Cohesive Zone Model

The cohesive zone model (CZM) is an emerging technology capable of simulating a crack formation and propagation. Thus, the advantage of the cohesive zone theory is it's not necessary to know where the crack is or will start. In CZM, interfacial separation occurs within a cohesive damage zone, when the damage exceeds a pre-set limit. Within a cohesive zone (CZ), there are active tensile stresses between surfaces. The interaction is governed by the law of tension separation. Before applying the load, a CZ element is declared healthy (no damage). A completely damaged element means the element was completely separated and does not produce any interaction force between the cohesive surfaces, reaching a damage value equal one. In Figure 3 is illustrated the interfacial separation of the CZM [2].

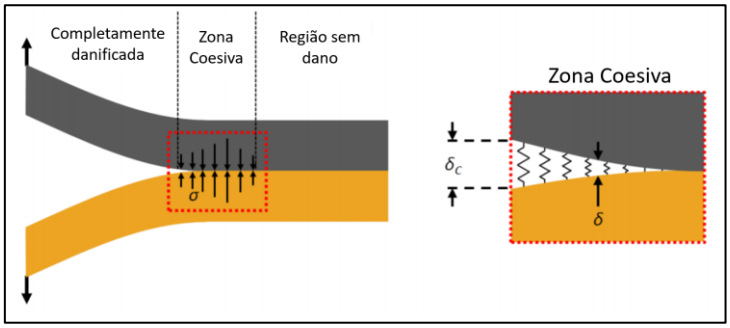

Figure 3 - Interfacial separation [2]

1.3. Bilinear traction-separation constitutive law

The bilinear tensile separation law was introduced in 2001 to model the interfacial separation. Several bimaterial interfaces were simulated using this law [7]. In Figure 4 is presented the bilinear law.

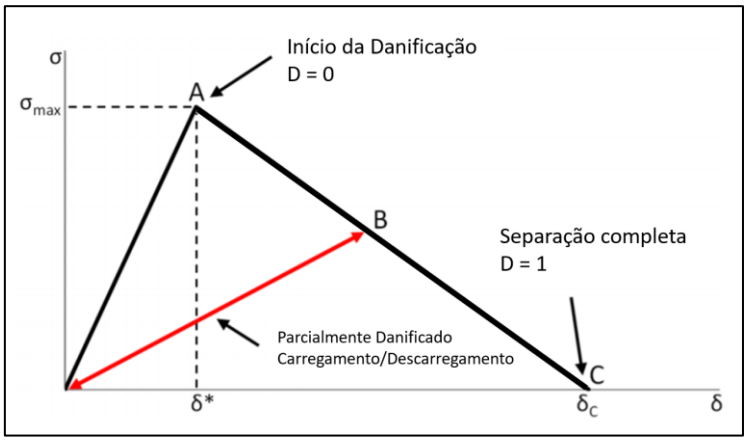

Figure 4 – Bilinear tensile separation law for cohesive zone elements [2]

The bilinear law is modeled by the tension (σ) as a function of the interfacial separation (δ). As the CZ elements suffer deformations, they present a linear behavior for δ < δ^*. In this curve region, no damage is accumulated at the interface and, consequently, unloading results in the CZ returning to original configuration. At point A, the critical tensile stress is reached (σ_{max}), and the damage process start. The detachment is monitored as a function of damage parameter (D), calculated by Eq.(1). When δ > δ^*, D increases and, when δ ≥ δc, D is maximum, that is, equal to 1.

$$D = \begin{Bmatrix} 0 \\ \left(\dfrac{\delta - \delta^*}{\delta}\right) \\ 1 \end{Bmatrix} \quad \begin{matrix} se\ \delta \leq \delta^* \\ se\ \delta^* < \delta < \delta_c \\ se\ \delta \geq \delta_c \end{matrix} \tag{1}$$

4 Methodology

The methodology adopted in this work is shown in Figure 5.

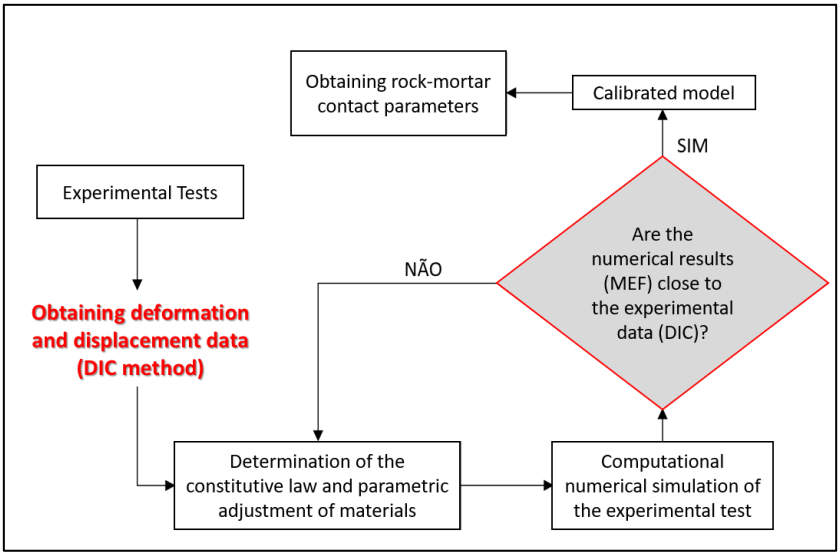

Figure 5 - Flowchart of the methodology adopted in this work

5 Case Study

According to the availability of the laboratory's infrastructure, it was possible to develop a rock-mortar interface detachment test under normal and shear stresses by a simple axial compression hydraulic press. Figure 6 shows the dimensions of the specimen in millimeters, as well as the materials of each component.

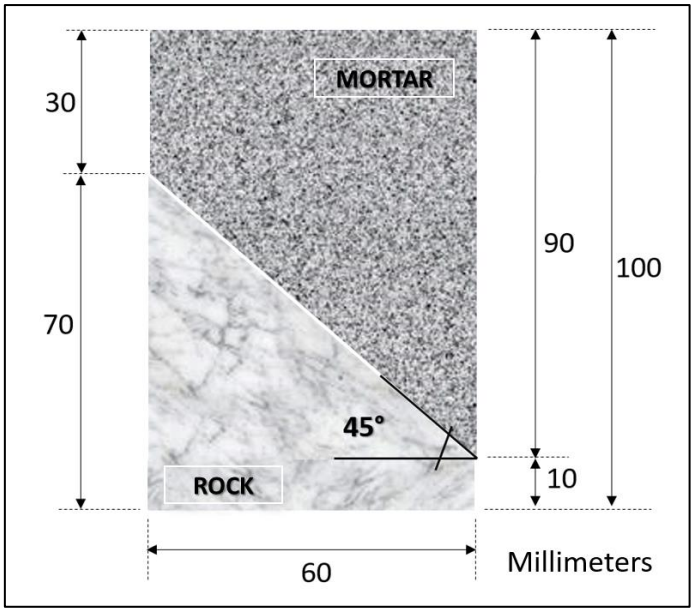

Figure 6 – Illustration of the rock-mortar test

The specimen is subjected to a controlled axial loading at the ends until the rupture of the rock-mortar contact by shear occurs, as shown in Figure 7.

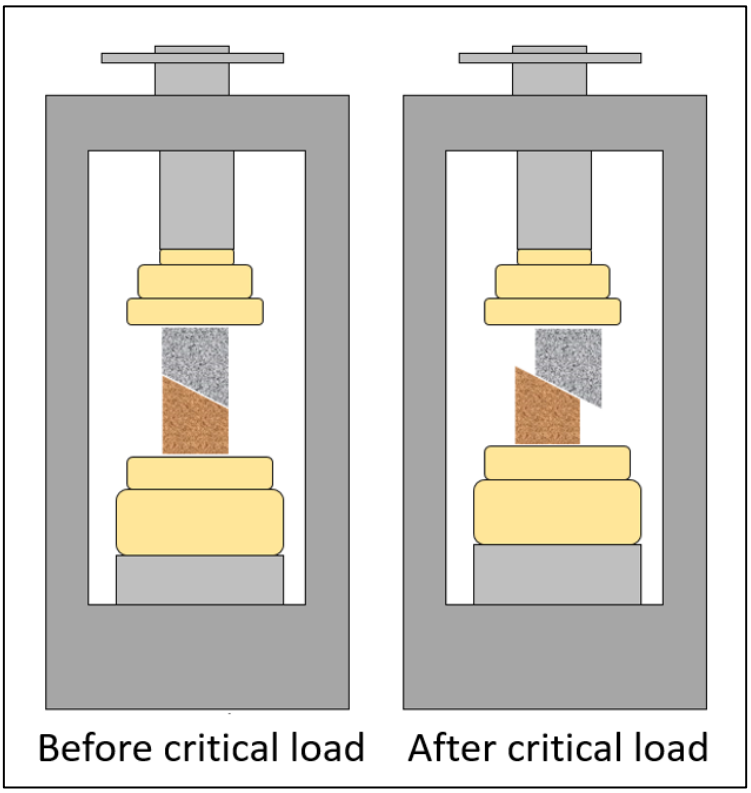

Figure 7 – Illustration of the breakage of the rock-mortar contact of the specimen

An example of a specimen after the mortar has hardened is shown in Figure 8

Figure 8 - Unmolded rock-mortar specimen

Following good test preparation practices for the application of the DIC method, initially, the specimens received a layer of white paint. Subsequently, black spray paint was used to create a random fine-grained texture (Figure 9).

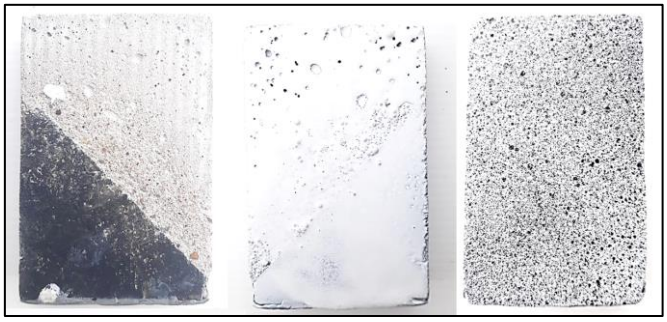

Figure 9 - Texture preparation of the rock-mortar specimens

The rupture test of the contact interface between rock and mortar was carried out using a Contenco analog hydraulic press. The test was monitored using a Sony Alpha a5000 digital camera (Mirrorless Digital Camera ILCE5000L/S), with 20.1 megapixels of resolution. In all, six tests were carried out on rock-mortar specimens (CP-RA). In two tests, there was a rupture of the mortar in the central region and a partial rupture of the rock-mortar contact interface (a). In two tests, the total rupture of the contact interface occurred smoothly (b) and, in two tests, the total rupture of the interface occurred abruptly (c), as shown in Figure 10.

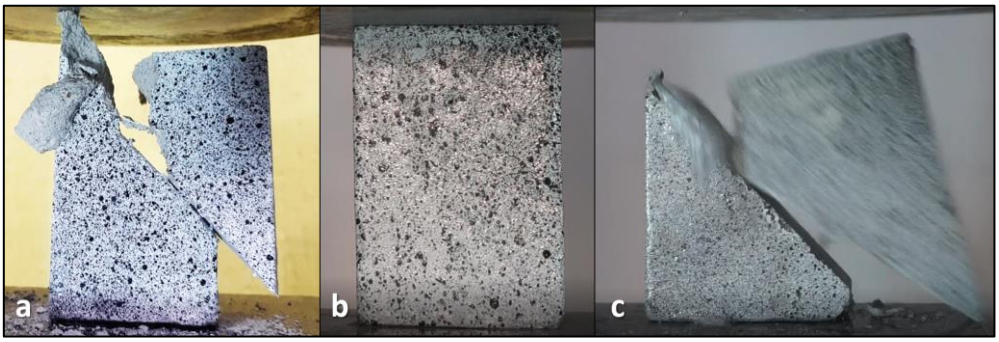

Figure 10 - Types of rupture obtained during the tests: partial rupture of the interface (a), smooth total rupture (b) and abrupt total rupture (c)

In Figure 11, the three monitoring points chosen in the specimens to collect displacement data of the images processed by the digital image correlation method are presented.

Figure 11 - Monitoring Points (DIC)

Figure 12 shows the results of processing moments before the CP-RA-02 test failure, using the GOM Correlate program.

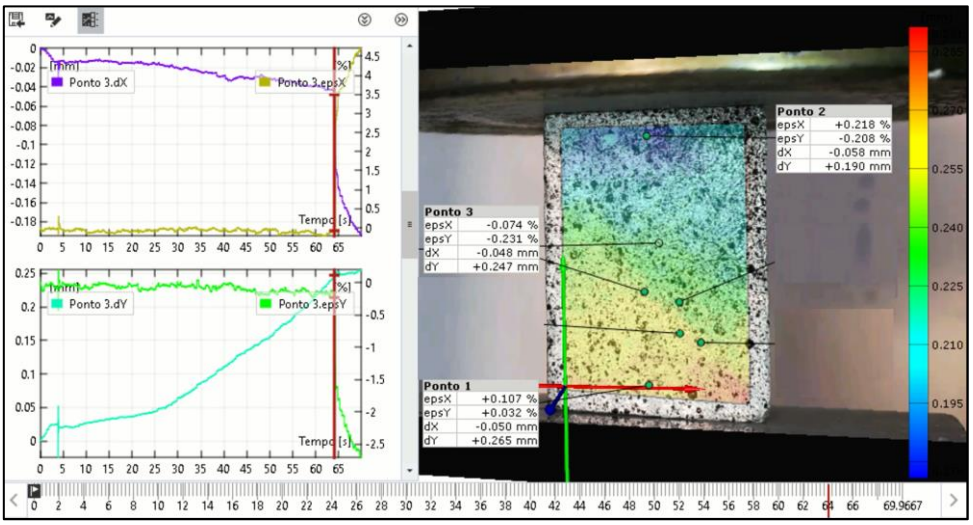

Figure 12 – CID results (vertical displacement field, monitoring points and point 3 displacement and deformation graphs) of the CP-RA-02 specimen.

In Graphs 1 to Graph 3, the displacement results in the vertical (y) and horizontal (x) directions of each monitoring point of CP-RA-02 are presented.

Graph 1 - Vertical and horizontal displacement of CP-RA-02 monitoring point 1

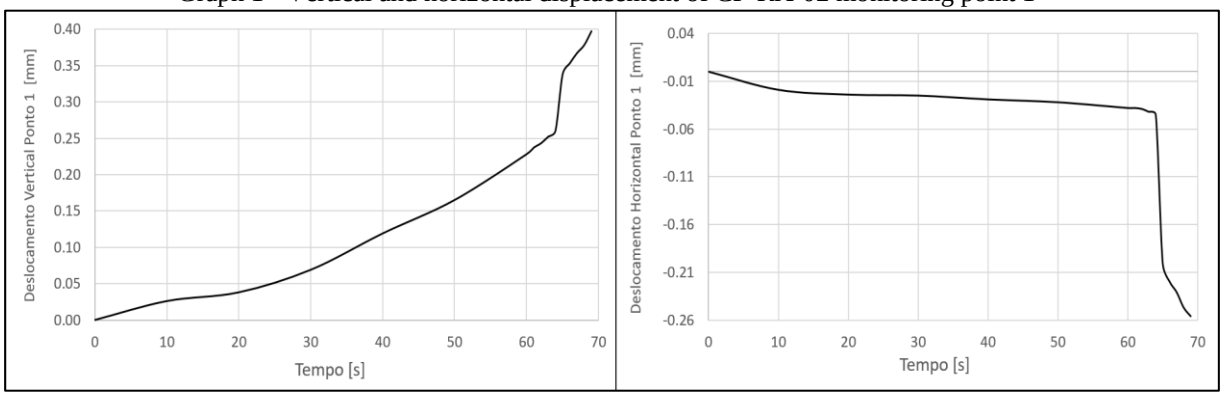

Graph 2 - Vertical and horizontal displacement of CP-RA-02 monitoring point 2

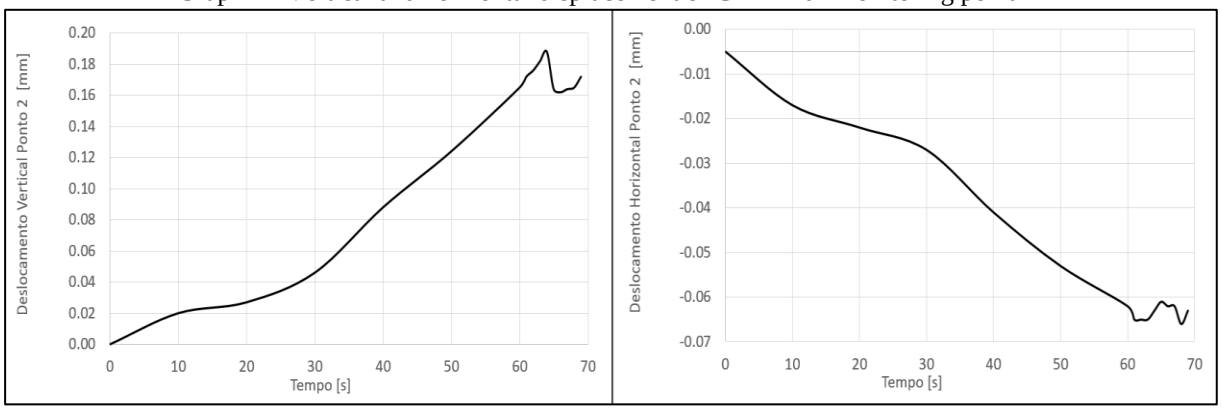

Graph 3 - Vertical and horizontal displacement of CP-RA-02 monitoring point 3

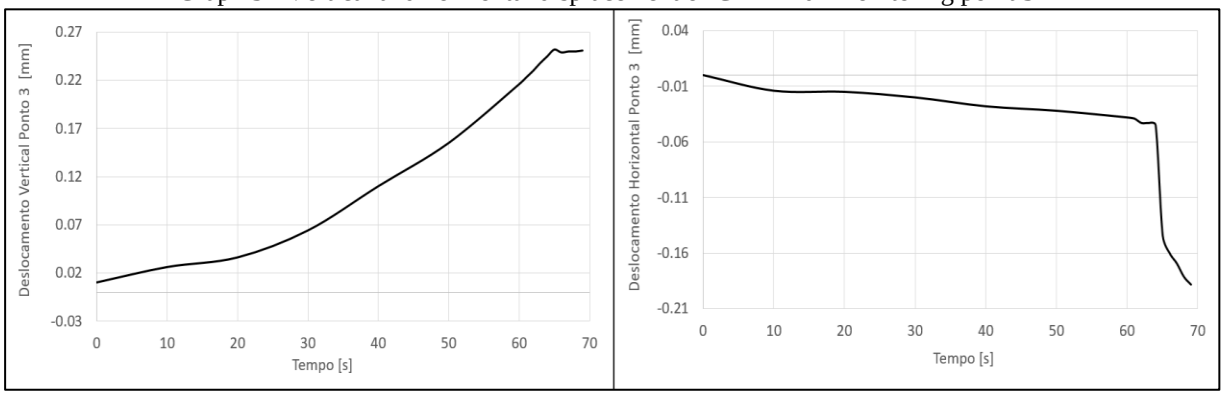

6 Numerical Simulation of Interfacial Rock and Mortar Rupture

For the development of the numerical failure model at the rock-mortar contact interface of the CP-RA-02 specimen, it was decided to use the Cohesive Zone Detachment method based on Separation Distance, similar to the Bilinear Law method. In this work, fracture mode II is predominant, since the contact interface is compressed all the time during the test. To perform the numerical analysis, it were adopted the material properties presented in Table 1.

Table 1- Material properties

Material	Modulus of elasticity [GPa]	Poisson's Coefficient	Density [Kg/m³]
Mortar	21*	0,2*	2350**
Rock	70*	0,25*	2650**

*Properties estimated through DIC results;
** Properties obtained from literature.

The mesh is formed by hexahedral elements, solid186. Altogether, the mesh consists of 18,775 nodes and 3,864 elements (Figure 37).

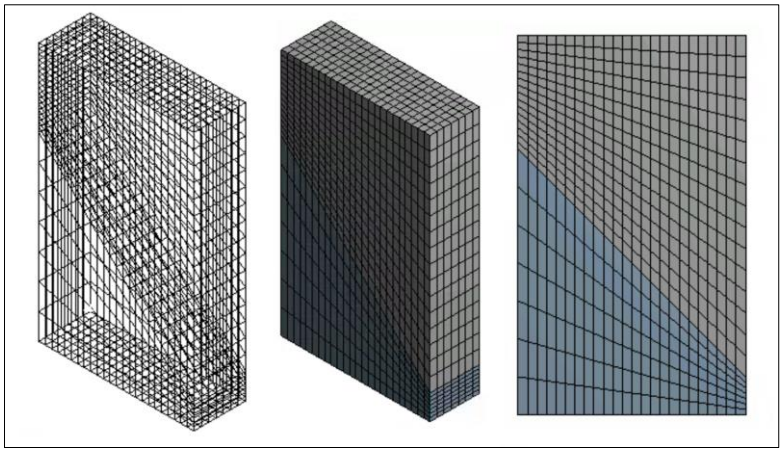

Figure 13 - Hexahedral mesh of the numerical model

To simulate the conditions of the hydraulic press, the fix support condition on the upper surface and loading on the lower surface were applied, as shown in Figure 14.

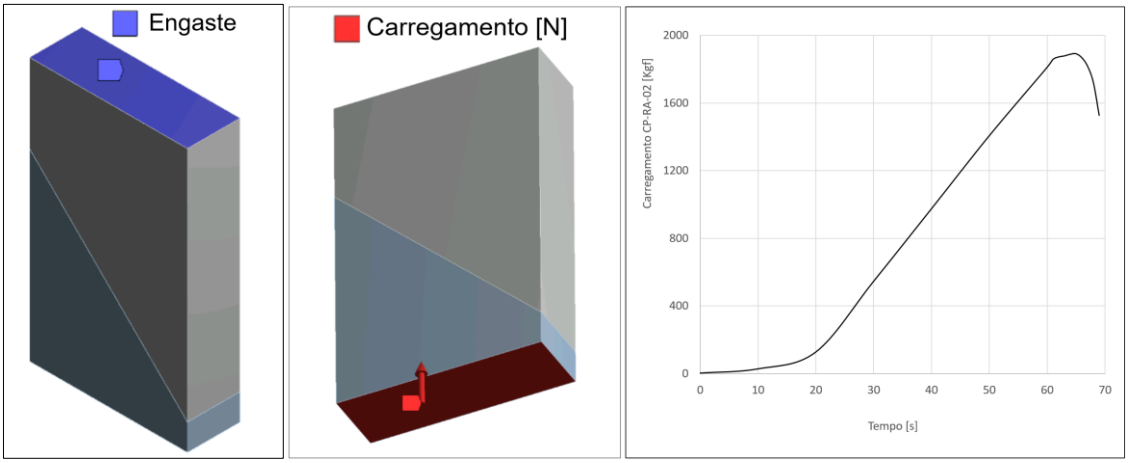

Figure 14 - Loading condition of the numerical model according to the experimental test

By the DIC method, aligning the reference coordinates towards the contact interface, it was found that the interface presented a slip of 0.206 mm, milliseconds before rupture, as shown in Figure 15.

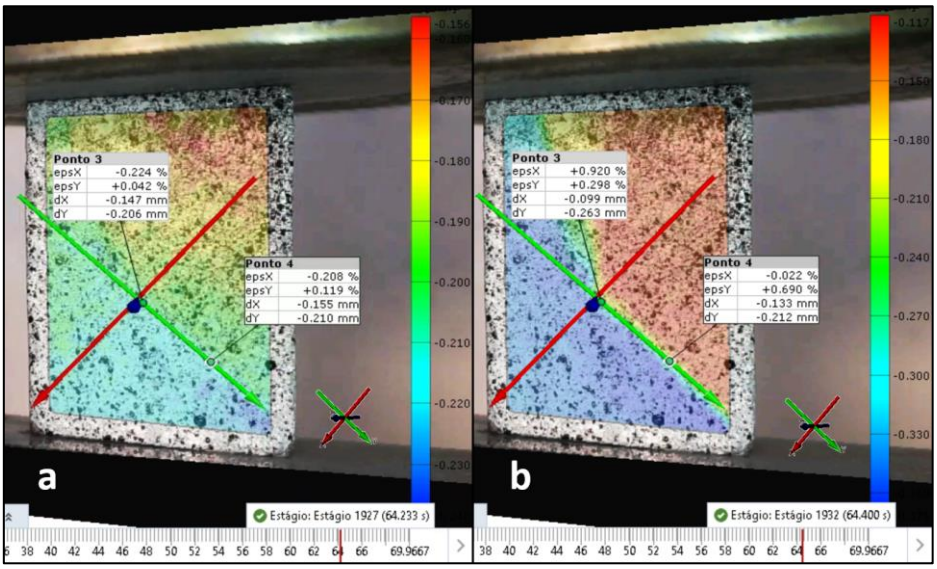

Figure 15 - Contact interface slip analysis obtained by DIC method

Finally, to start the nonlinear analysis and define the cohesive zone parameters through the bilinear law, the rupture displacement equal to 0.2 mm was defined, as presented in the experimental test and monitored by the DIC method (Figure 15). Figure 16 shows the partially developed Bilinear Law for Cohesive Zones.

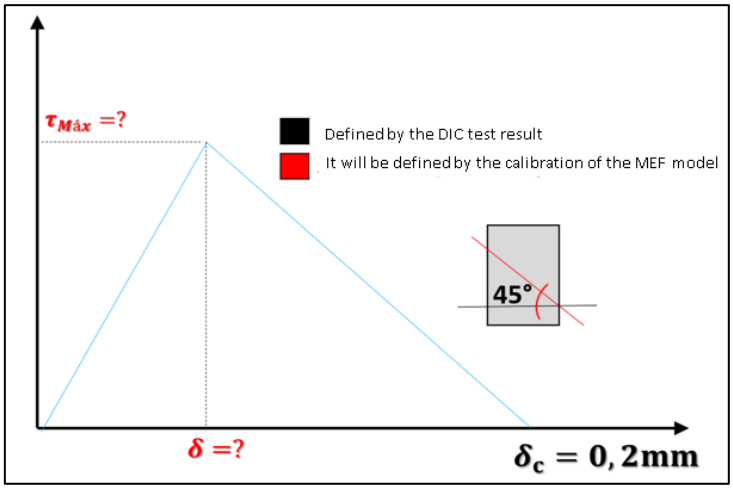

Figure 16 - Graphic illustration of the Bilinear Law partially defined

To define the remaining properties of the bilinear law, a parametric analysis was performed, varying the maximum shear stress until the model rupture to occur at time t=64.2s. The Table 2 presents the main results of the parametric analysis until obtaining the expected behavior of the numerical model and calibrating with the experimental DIC results.

Table 2 - Summary of the parametric analysis performed to calibrate the numerical model

Nº	$\tau_{máx}$ [MPa]	$\delta_{máx}$ [mm]	Damage start time [seg] ($\tau_{contato} > \tau_{máx}$)	Total break time [seg] ($\delta_{contato} > \delta_{máx}$)
1	11,3	0,2	60	-
2	10	0,2	55	-
3	8	0,2	48	67
4	7,5	0,2	46	66
5	7,2	0,2	45,5	64,4
6	**7,15**	**0,2**	**45,4**	**64,2**

In Figure 17 to Figure 21, the vertical displacement (Y), experimental test (DIC) and numerical model (FEA) fields are shown, respectively.

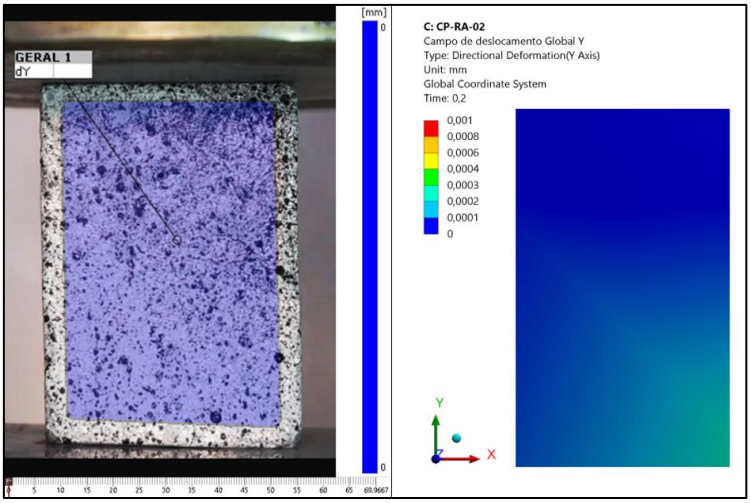

Figure 17 - Test vertical displacement field (DIC) and numerical model (t=0s)

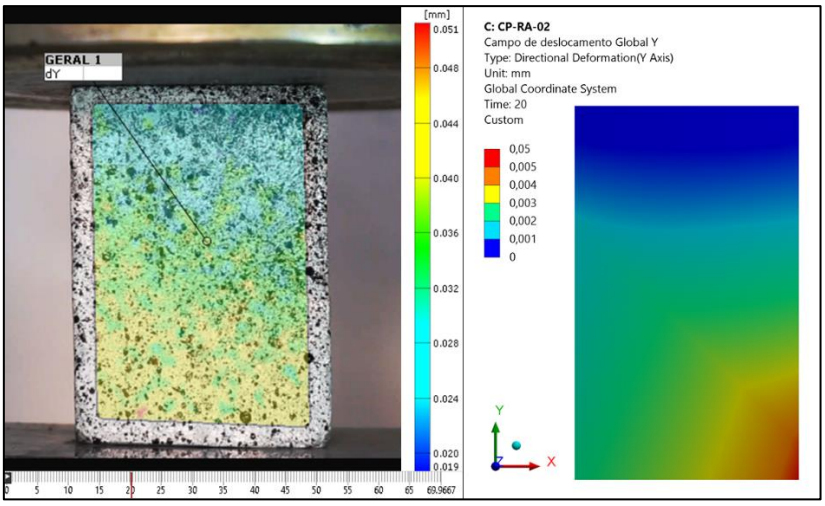

Figure 18 - Test vertical displacement field (DIC) and numerical model (t=20s)

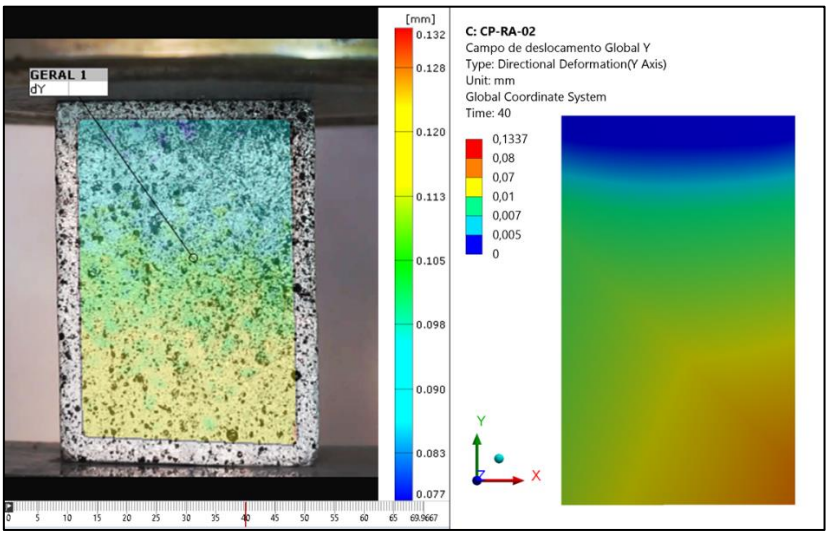

Figure 19 - Test vertical displacement field (DIC) and numerical model (t=40s)

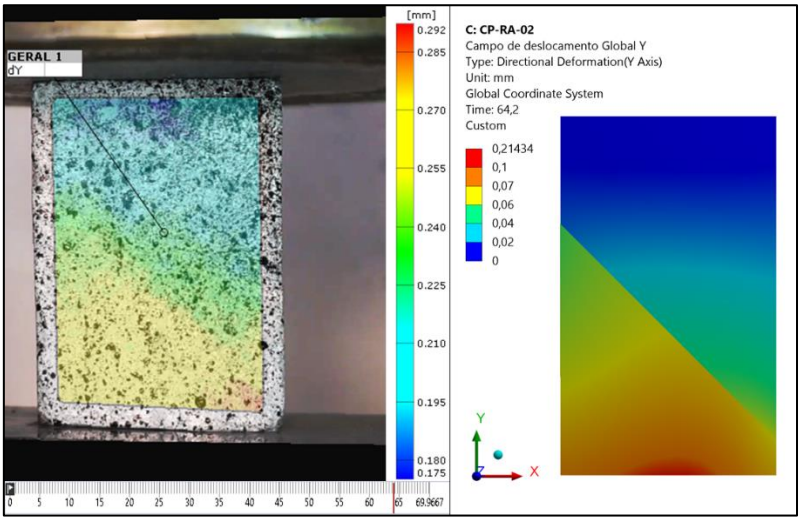

Figure 20 - Test vertical displacement field (DIC) and numerical model (t=64,2s)

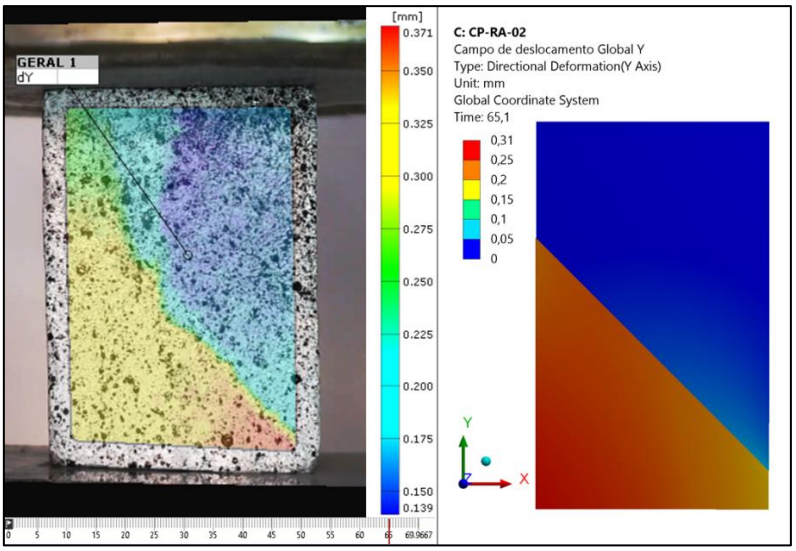

Figure 21 - Test vertical displacement field (DIC) and numerical model (t=65,1s)

In Figure 22 to Figure 26, the fields of horizontal displacement (X), the experimental test (DIC) and the numerical model are presented.

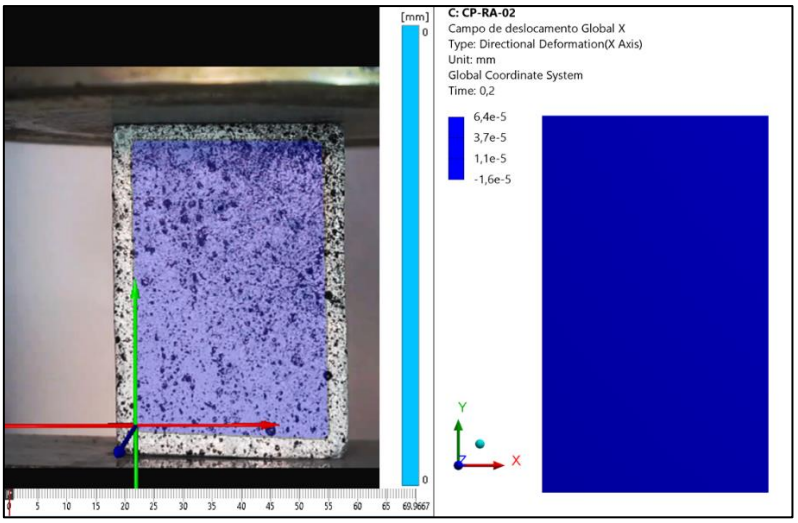

Figure 22 - Test Horizontal Displacement Field (DIC) and Numerical Model (t=0s)

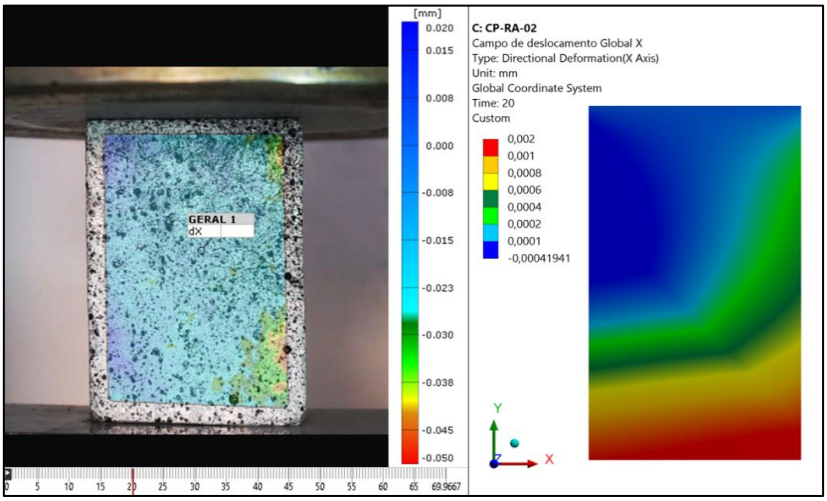

Figure 23 - Test Horizontal Displacement Field (DIC) and Numerical Model (t=20s)

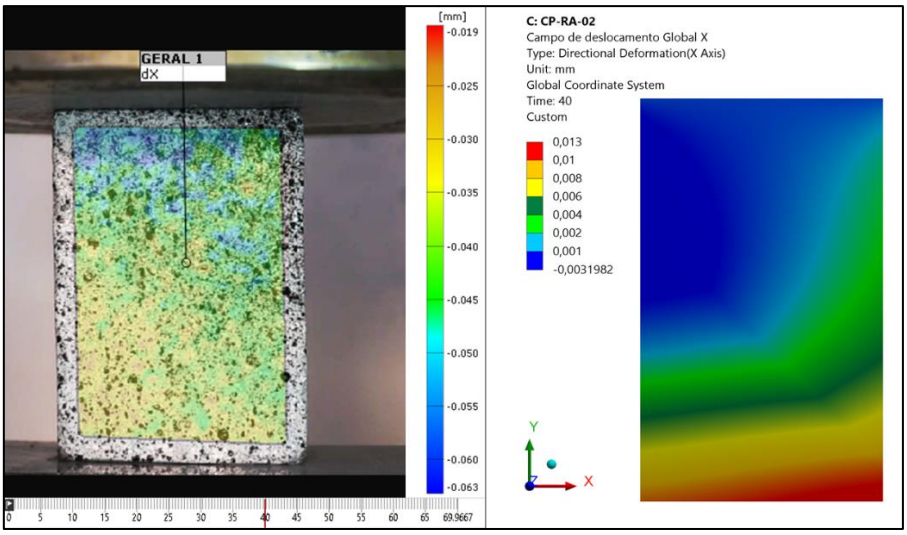

Figure 24 - Test Horizontal Displacement Field (DIC) and Numerical Model (t=40s)

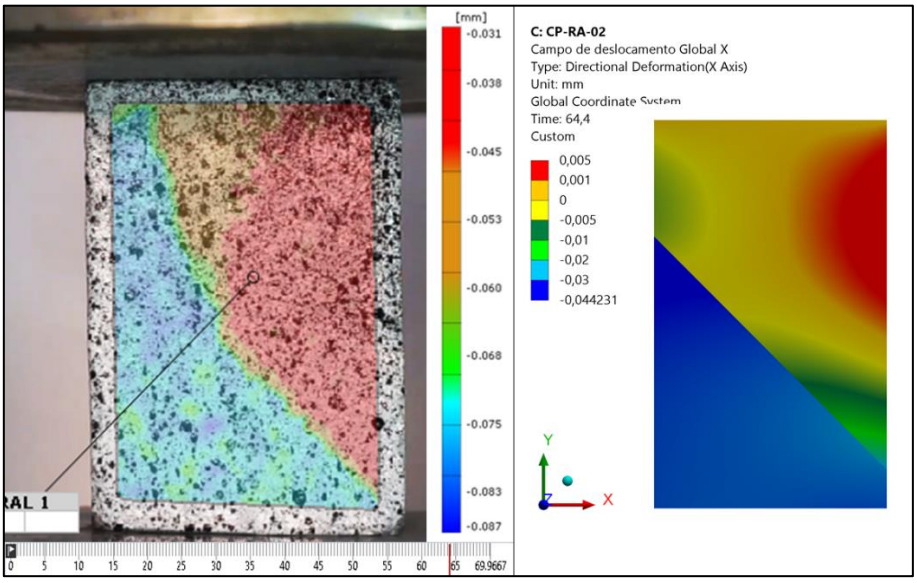

Figure 25 - Test Horizontal Displacement Field (DIC) and Numerical Model (t=64,2s)

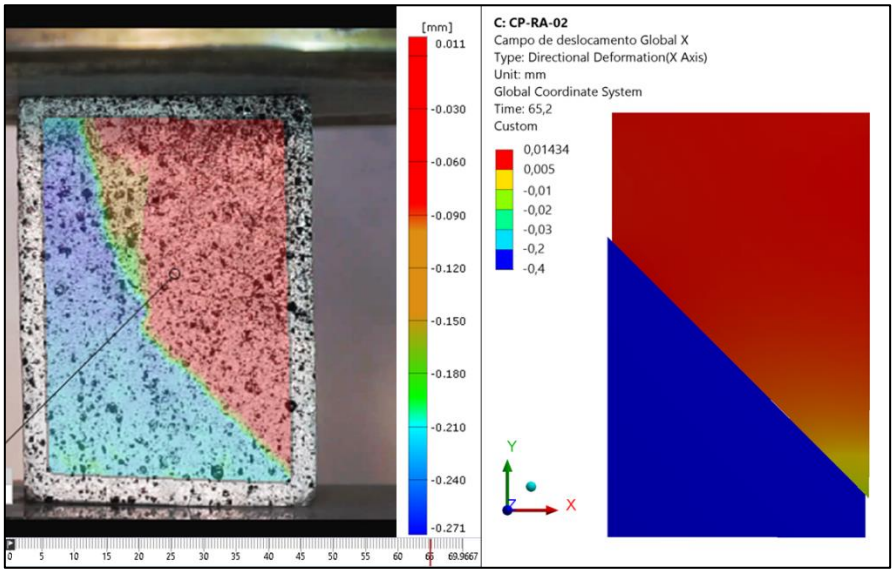

Figure 26 - Test Horizontal Displacement Field (DIC) and Numerical Model (t=65,1s)

Figure 27 to Figure 28 show the normal stress fields, vertical (Y) and horizontal (X), of the numerical model.

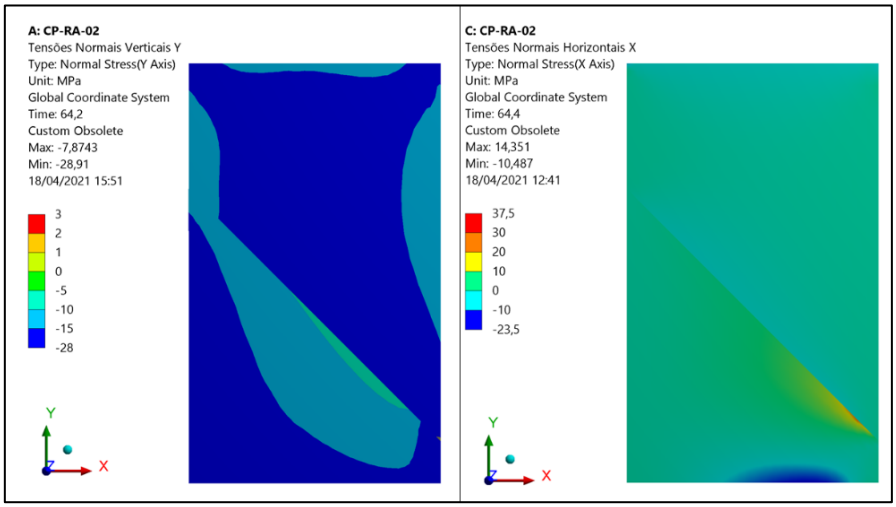

Figure 27 - Field of normal stresses of the numerical model, vertical e horizontal (t=64,2s)

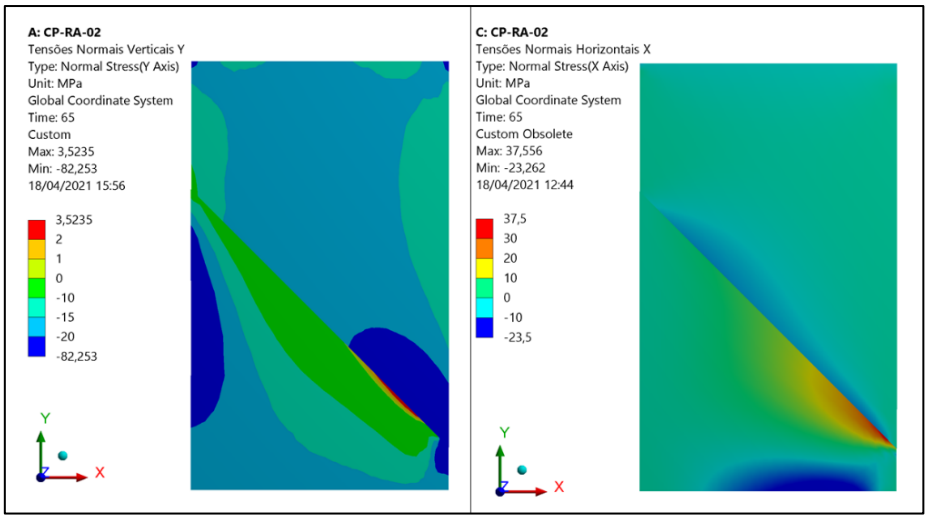

Figure 28 - Field of normal stresses of the numerical model, vertical e horizontal (t=65s)

The analysis of the monitoring points of the experimental test was carried out and compared with results from the same points of the numerical model. Graphic illustrations of the monitoring points, DIC and FEA, are shown in Graph 4 to Graph 6.

Graph 4 - Vertical and horizontal displacements of monitoring point 1

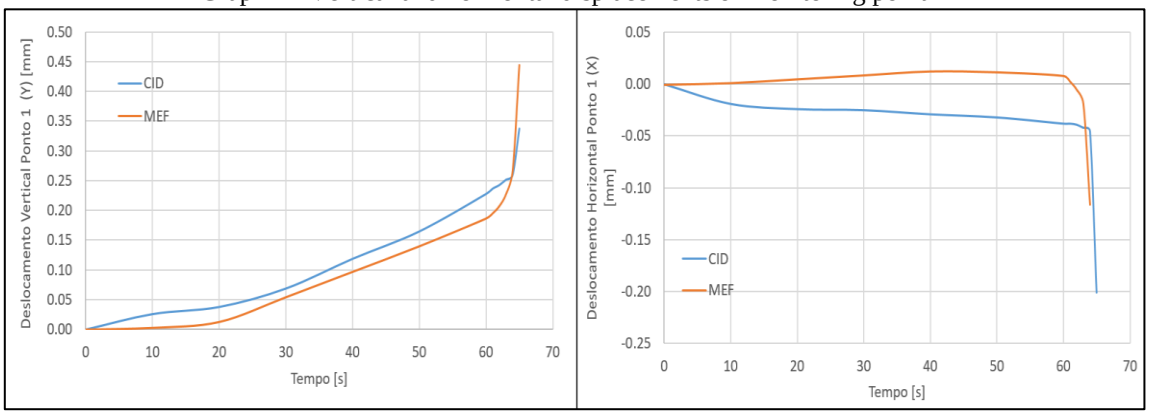

Graph 5 - Vertical and horizontal displacements of monitoring point 2

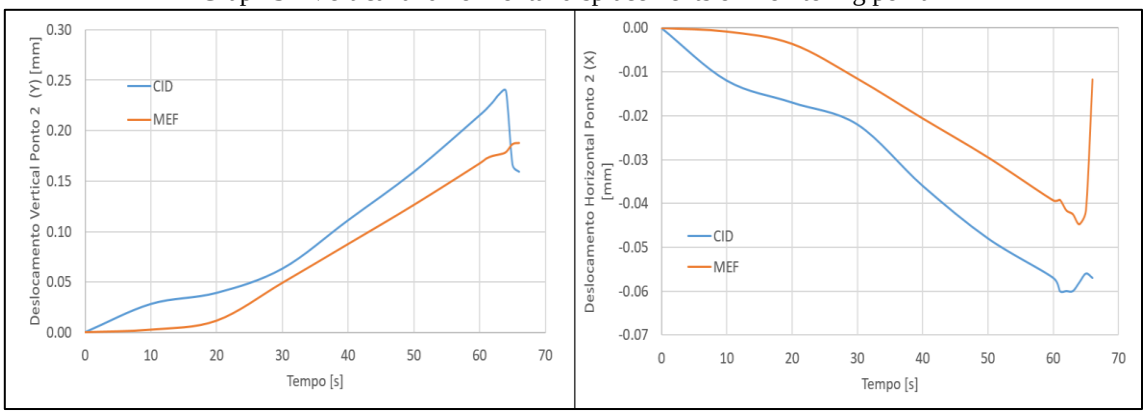

Graph 6 - Vertical and horizontal displacements of monitoring point 3

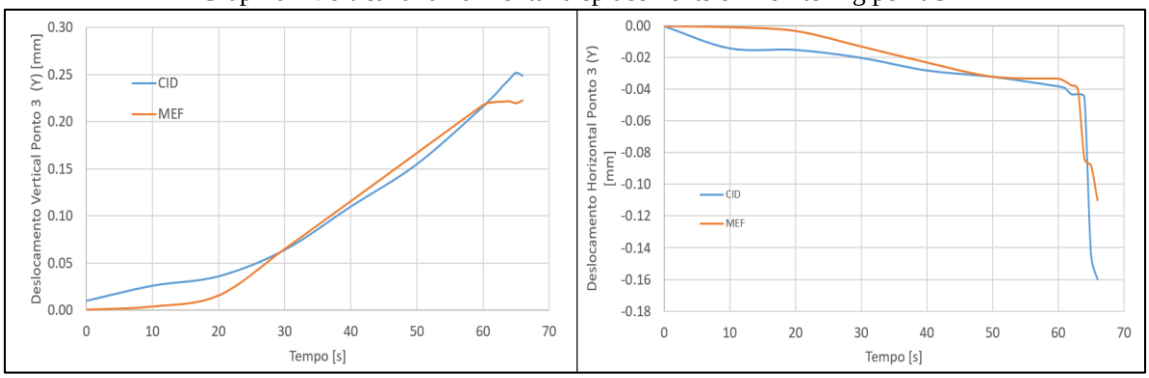

The analysis of the accumulated percentage difference of the DIC and FEA results was carried out through the Mean Absolute Percentage Error (MAPE - Mean Absolute Percentage Error). Table 7 shows the MAPE values for each monitoring point.

Table 7 - MAPE error of monitoring points

Monitored point	1		2		3	
Displacement direction	x	y	x	y	x	y
MAPE Error	-	11.77	36.59	19.5	5.94	3.06

6.1 Contact Interface Behavior (Cohesive Zone - Bilinear Law)

Calibrating the numerical model with the CZM properties presented in Table 2, it can be seen in Graph 7 and Figure 29(a), the nonlinear behavior in the contact starts at the same moment that the maximum shear stress of the interface reaches the maximum value of the shear Bilinear Law, 7.15 MPa (t=45.4s).

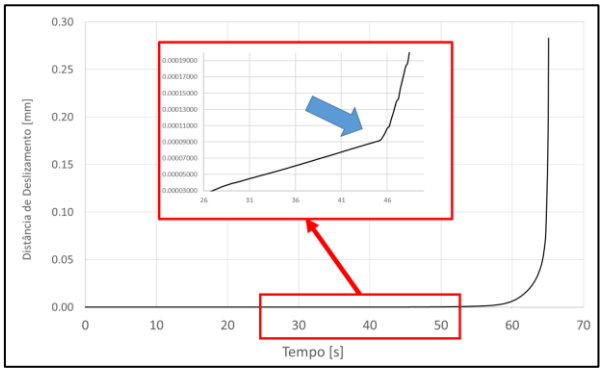

Graph 7 - Sliding of the contact and detail interface when non-linear behavior starts

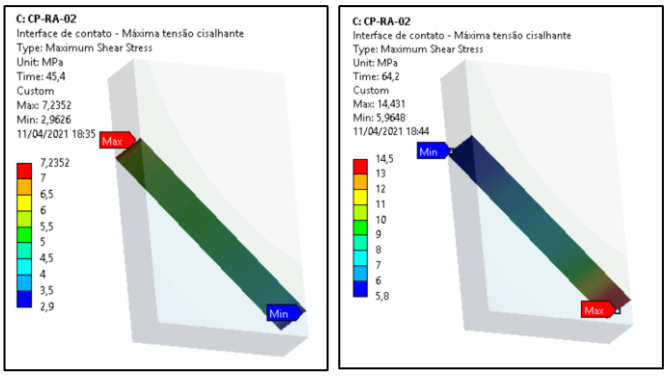

Figure 29 - Maximum shear stress field at the contact interface: (a) t=45.4s and (b) t=64.2s

Thus, from time t=45.4s, the process of damage to the contact elements began. The total breakage of the contact occurs at time t=64.2s, when most of the contact elements reach the maximum displacement provided for in the Bilinear Law of 0.2 mm. Analyzing the maximum shear stress field at the contact interface, it is observed that the region with the highest value moves from the upper left region (t=45.4s) to the lower right region (t=64.2s) . At the failure moment, the contact interface has a maximum shear stress of 14.5 MPa, as shown in Figure 29(b). This is because, with the beginning of the detachment of the contact interface, the distribution area of stress decreases. In this way, the shear stress increases at the same speed as the contact detachment occurs, until total rupture.

6.2 Cohesive Zone Parameters Determination

According to Alfano and Crisfield (2001), the bilinear law is defined by three parameters: maximum stress, critical displacement and loading and unloading rate. The latter is obtained through the relationship between the displacement that initiates the damage and the critical displacement. Analyzing Graph 7, it is possible to observe that the damage starts when the contact element reaches the maximum shear stress $\tau_{max} = 7{,}15\ MPa$ and displacement $\delta^* = 9x10^{-5}\ mm$. Thus, the parameters of the Bilinear Law that simulate the behavior of the rock-mortar cohesive interface of the CP-RA-02 test (with a 45º contact interface inclination angle) are presented in Table 4.

Table 4 – Bilinear Parameters Law

$\tau_{max}\ [Mpa]$	7,15
$\delta_c\ [mm]$	0,2
δ^*/δ_c	0,00045

The graphic illustration of the complete Bilinear Law is shown in Figure 30.

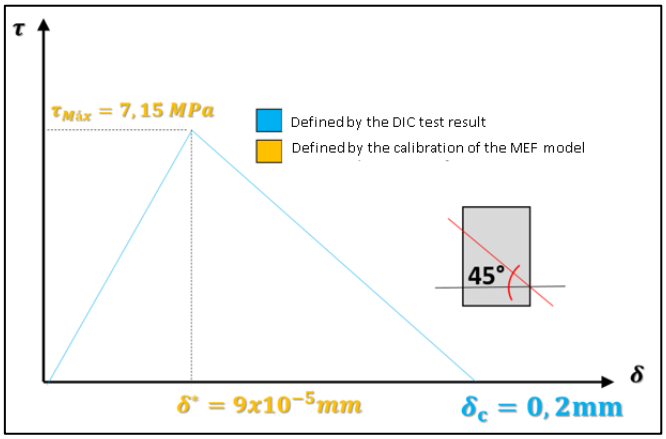

Figure 30 – Graphic illustration of the bilinear law complete with data from the DIC and FEA method.

When a finite element begins to break down, the area below the tensile separation law function accounts for the mechanical work required to separate the element. Thus, the area under the curve is equivalent to the Gc (critical rate of deformation energy release of linear elastic fracture mechanics) [2]. Using the parameters of the Bilinear law, Gc can be estimated using Eq.(2).

$$G_c = \frac{1}{2}\delta_c \sigma_{max}. \tag{2}$$

Thus, the Gc parameter is equal to 0.71 [N/mm].

7 Conclusion

In this work, in order to register the abrupt phenomenon of contact interface displacement, it was necessary to perform the video recording of the experimental test. This decision impacted the DIC processing phase. Using a computer with 56 GB RAM memory and Intel i5 3.50 GHz processor, the processing time of the tests performed was 40 to 60 minutes. The first parameter to calibrate the numerical model was obtained by the DIC method, aligning the reference coordinates towards the contact interface. Thus, it was found that the interface presented a slip of 0.206 mm, milliseconds before rupture. Regarding the non-linear numerical contact model, after evaluating all cohesive zone methods available in the Ansys material library, we chose to use the Law of Detachment based on the Separation Distance. This method requires fewer calibration parameters and allows configuration to Mode I, Mode II or Mixed Fracture Mode. Then, a parametric analysis was performed, varying the maximum shear stress of the CZ contact elements to calibrate the numerical model considering the exact rupture time of the test as one of the requirements for the simulation validation. Using the CZ parameters presented in Figure 30, the numerical model started the process of contact element damage at time t=45.4s, when it reached the maximum shear stress foreseen in the bilinear law (7.15Mpa). The total contact breakage occurred at time t=64.2s, when most of the contact elements reached the maximum predicted displacement of 0.2 mm. Overall, the difference accumulated in the entire test is considered satisfactory, especially in the region of the contact interface where the MAPE error for the horizontal displacement was 5.94% and the vertical, 3.06%. Finally, with the model considered calibrated, the Bilinear Cohesive Zone Law was defined for the particular case of a 45º contact interface between rock and mortar tested in the laboratory.

Acknowledgements. We would like to thank the Federal University of Latin American Integration (Unila) for financing of this work, and the Itaipu Technological Park for the technological resources for the preparation of this work.

The authors hereby confirm that they are the sole liable persons responsible for the authorship of this work, and that all material that has been herein included as part of the present paper is either the property (and authorship) of the authors, or has the permission of the owners to be included here.

References

[1] ALMEIDA, G. Image Processing for Displacement Measurements. Tese de Doutoramento. FCT-UNL, 2014. Disponível em: < https://run.unl.pt/bitstream/10362/14595/1/Almeida_2014.pdf>. Acessado em: 15 set. 2020.

[2] KRIEGER, W. E. R. Cohesive Zone Modeling For Predicting Interfacial Delamination in Microelectronic Packaging. Thesis. Georgia Institute of Technology. 2014.

[3] SUTTON, Michael, A, ORTEU, Jean J, SCHREIER, Hubert W. Correlation for Shape, Motion and Deformation Measurements: Basic Concepts, Theory and Applications. Springer Science. 2009. [4] Beleza (2017),

[5] JUNIOR, E. B. Utilização do Método de Correlação de Imagens na Caracterização de Materiais Metálicos e Poliméricos. Dissertação de Mestrado. Universidade Federal Fluminense. 2008.

[6] SILVA, Angelo Q. N. Correlação de Imagens Digitais em Ensaios de Compressão Diametral em Rochas. Tese de doutorado. UNIVERSIDADE FEDERAL DE MINAS GERAIS.

[7] ALFANO, G.; CRISFIELD, M. Finite Element Interface Models for The Delamination Analysis of Laminated Composites: Mechanical and Computational Issues. International journal for numerical methods in engineering. Vol. 50. 2001.

[8] WEI, D.; ZHIMIN W.; XIANG; M. Z.; NA, W.; Kastiukas, G. An experimental study on crack propagation at rock-concrete interface using digital image correlation technique. Engineering Fracture Mechanics. Elsevier. 2016.